NASA Technical Memorandum 101357
AIAA-88-3152

Euler Analysis of a Swirl Recovery Vane Design for Use With an Advanced Single-Rotation Propfan

Christopher J. Miller
Lewis Research Center
Cleveland, Ohio

Presented at the
24th Joint Propulsion Conference
cosponsored by the AIAA, ASME, SAE, and ASEE
Boston, Massachusetts, July 11-13, 1988

NASA

EULER ANALYSIS OF A SWIRL RECOVERY VANE DESIGN FOR USE WITH AN ADVANCED SINGLE-ROTATION PROPFAN

Christopher J. Miller
National Aeronautics and Space Administration
Lewis Research Center
Cleveland, Ohio 44135

SUMMARY

Recent work has demonstrated the propulsive efficiency improvements available from single- and counter-rotation propfans as compared with current technology high bypass ratio turbofans. This paper examines the concept known as swirl recovery vanes (SRV) through the use of a three-dimensional Euler code. At high speed cruise conditions, the SRV can improve the efficiency level of a single-rotation propfan, but a concern is to have adequate hub choke margin. The SRV was designed with two-dimensional methods and was predicted to have hub choking at a Mach 0.8 cruise. The three-dimensional Euler analysis properly accounts for sweep effects and three-dimensional relief, and predicts that at cruise the SRV will recover roughly 5 percent of the 10 percent efficiency loss due to swirl and have a good hub choke margin.

INTRODUCTION

The high speed propfan technology began with single-rotation configurations and progressed to counter-rotation propfans, which are more efficient because they recover the swirl losses associated with high power loadings. For some applications the complexity, cost, or weight of a counter-rotation installation is prohibitive. An advanced concept currently being investigated is the use of a row of nonrotating vanes behind a single-rotation propfan. These swirl recovery vanes can recover a significant fraction of the swirl loss and thereby approach the efficiency of a counter-rotation propfan, but are a much simpler system. This paper presents an Euler analysis of a preliminary experimental design developed to study the interaction between the propfan and SRV, with the intent of verifying the overall design concepts.

Single-rotation propfan performance has been studied for many different geometries. For one of these, the NASA SR-3, detailed experimental data exists at high speed conditions (refs. 1 and 2). The cruise design point for this eight bladed propfan is: a freestream Mach number of 0.8, an altitude of 10.68 km (35 000 ft), a tip speed of 243.8 m/sec (800 ft/sec) and a power loading of 301 kW/D^2 (37.5 shp/D^2). At corresponding wind tunnel conditions, the model propeller achieved a net efficiency of 78.2 percent. It is currently believed that the poor spinner design leads to compressibility losses in the blade root region which, at the design point, amounts to about a 2 percent loss in efficiency (3). Thus, an improved hub design would be expected to raise the net efficiency to roughly 80 percent at this design point. Net efficiency variation with Mach number is shown in figure 1, which is taken from reference 3, for the model SR-3 as tested and with an estimate for hub losses removed.

Counter-rotation propfan performance testing is a relatively new field for which limited performance data exists. One example of a counter-rotation configuration that was tested at high speed is the CRP-X1 propfan (ref. 3). The design point for this 5 by 5 bladed propfan is: a freestream Mach number of 0.72, an altitude of 10.68 km (35 000 ft), a tip speed of 228.6 m/sec (750 ft/sec) and a power loading of 298.2 kW/D^2 (37.15 shp/D^2). Figure 1 also shows the variation of net efficiency with Mach number at the design C_P and tip speed for the CRP-X1. As tested, there is a 7 percent difference in efficiency (5 percent without SR-3 hub losses) at Mach 0.8 and a slightly larger difference at Mach 0.72.

While a counter-rotation configuration has a net efficiency advantage over a single-rotation design of the same power loading, it also has an attendant increase in complexity and cost. A single-rotation propfan with swirl recovery vanes provides an option between single- and counter-rotation both in cost and performance. Low-speed analytical (refs. 4 and 5) and experimental (ref. 6) work on swirl recovery from the interaction between propellers and wings has predicted and demonstrated that large beneficial interactions are available. It is possible to use propfan-wing interactions to recover swirl at high speeds, but the wing, having only two "blades," will not do it efficiently.

A major concern with the use of swirl recovery vanes in high power loading-high speed conditions is the possibility of SRV blade root choking. With the SR-3 spinner the loss was approximately 2 percent in efficiency. For a SRV recovering roughly 5 percent in efficiency, similar compressibility losses would be a severe penalty. It is therefore important to accurately access the blade performance. The three-dimensional multi-row Euler analysis is used to compare the three-dimensional configurations because it provides more and better information than the coupled use of through flow and passage analyses. This work is an attempt to validate the efficiency benefit of the SRV concept and to identify whether choking is a problem in the preliminary SRV design.

SYMBOLS

C_T thrust coefficient = $T/(\rho n^2 D^4)$

C_P power coefficient = $P/(\rho n^3 D^5)$

J advance ratio = $V_0/(nD)$

D propeller diameter

n revolutions per second

N_a number of chordwise (axial) grid points

N_r number of spanwise (radial) grid points

N_c number of grid points in a blade passage

V_0 freestream (axial) inflow velocity

T thrust

P power

η propeller efficiency = JC_T/C_P

ρ freestream air density

GEOMETRY

In an effort to develop SRV technology for high speed propfans, a preliminary swirl recovery vane system was designed under contract to be operated downstream of the eight bladed single-rotation SR-3. The SR-3/SRV design point is at Mach 0.8, with a power loading of 321 kW/D^2 (40 shp/D^2) at 35 000 ft. This is an increase in power loading from the original SR-3 value of 301 kW/D^2 (37.5 shp/D^2) at 35 000 ft. Details of the SR-3 design are in reference 1. The SRV has 12 highly loaded and slightly tapered vanes. The vanes are fixed pitch with very low twist and NACA 16 series airfoil sections.

The body geometry is significantly different than that of the original SR-3. The SR-3 spinner and propeller are the same as the original, but behind the SR-3 the hub contour is changed: from the point of maximum diameter aft the wasp-waist is changed to a constant diameter cylinder. This allows for two axial positions of the SRV: a near position at about 35 percent of the SR-3 diameter from the pitch change axis (PCA) of the SR-3 to the PCA of the SRV, and a far position at about 66 percent of the SR-3 diameter from PCA to PCA. The blade and vane pitch settings are also adjustable. The geometry of the test rig for high speed wind tunnel testing is shown in figures 2 and 3 at the near and far spacing positions.

ANALYSIS METHOD

The Euler code used for these studies is that developed by Adamczyk et al. (refs. 7 and 8). This code solves for the three-dimensional flow through an "average" passage of a blade row. The solution of a multiple row machine is handled through an inner and outer loop procedure. The inner loop uses a modified Jameson finite volume scheme with Runge-Kutta integration to solve for the flow through a single blade row. The other row(s) during this calculation are represented by distributed body forces, energy sources and correlations applied to the cells swept out by those rows. Once the inner loop converges, the axisymmetric average of the inner loop solution is used to update the body forces, energy sources and correlations used to model that row when calculating the flow through the other row(s). The outer loop cycles through the blade rows until the mean squared difference between the axisymmetric flow solutions falls below a given tolerance. Comparisons of experimental data with calculations from this code for a high speed counter-rotation propfan show good agreement (ref. 9).

RESULTS

The analysis of the SRV began with a grid sensitivity study. To simplify this study, all meshes had the same physical far field boundary locations and each had the same number of points on the blade axially (chordwise), as well as spanwise and in a blade passage. The inflow boundary is physically located roughly 1.5 SR-3 tip radii upstream of the SR-3. The radial boundary is at about 2.5 SR-3 tip radii, and the outflow boundary is about 1.5 SR-3 tip radii downstream of the SRV. Figure 4 shows the (axial, radial) coordinates of the 7:7:7 mesh.

The mesh density away from the blades scales axially with N_a, and radially with N_r, so the N's effect the mesh globally. The study was done with the SRV at the far spacing for values of $N_a:N_r:N_c$ = 7:7:7, 9:9:9, 13:13:13, and 17:17:17. The meshes are in a cylindrical coordinate system and are axisymmetric, i.e., changing the circumferential index only changes theta, not the axial or radial position. Details of the meshes are listed below.

Mesh Parameters	Values			
N_a	7	9	13	17
N_r	7	9	13	17
N_c	7	9	13	17
Total axial points	55	63	109	125
Total radial points	14	17	27	33
Total azimuthal points	7	9	13	17
Blade tip grid index	7	9	13	17
SR-3 leading edge index	12	13	23	25
SR-3 trailing edge index	18	21	35	41
SRV leading edge index	40	45	79	89
SRV trailing edge index	46	53	91	105

The effect of grid density on the overall performance parameters (thrust coefficient, power coefficient, and efficiency) gives a quantitative measure of convergence to the solution for an infinite number of grid points. The effect on power coefficient and efficiency is presented in figure 5 for the design point conditions of a Mach 0.80 inflow, an advance ratio of 3.26 and a power loading of roughly 321 kW/D^2 at 35 000 ft. The fixed SR-3 geometry does not absorb a constant power because of the affect of the SRV. The rotational speed, n, and diameter, D, of the SR-3 are used in calculating all values of C_T and C_P.

To calculate system performance, the sum of the SR-3 and SRV thrust is used in calculating the thrust coefficient and efficiency. Referring again to figure 5, while the finest mesh, 17:17:17, does not yield the asymptotic values, it seems adequate for this study. More importantly, the system efficiency is converging with mesh density, so it appears that the finer meshes are not demonstrating evidence of compressibility related losses.

Figure 6 shows the suction surface absolute Mach number contours on the SR-3 propfan for two mesh densities: 13:13:13 and 17:17:17 with the SRV at the

far position. Absolute Mach number is used because it enhances the differences, although relative Mach number would normally be shown because it is the flow field seen by the moving blade. The differences between the two solutions are small. The contours for the finer mesh show a stronger shock outboard near the trailing edge, and at the hub the velocities are slightly lower.

The pressure surface contours show even less change than those on the suction surface. For this reason, the pressure surface contours will not be shown for any of the cases.

A similar mesh effect comparison is shown in figure 7 where the Mach contours on the SRV are shown for the 13:13:13 and 17:17:17 mesh densities. (Absolute and relative Mach number are the same on nonrotating bodies.) With the finer mesh, the outboard sonic region is about twice as large in the axial and spanwise directions. Also the finer mesh has only a single grid point near the hub where the flow is above Mach 1.0. There are no major changes in the Mach contours, nor is there evidence of choking at the hub. Figure 8 presents a radial plane one grid line off the hub surface with Mach contours in the SRV blade passage. Again there are small differences due to mesh density, but there is no evidence of choking.

The effect of the SRV on the SR-3 propfan absolute Mach contours is shown in figure 9 as a function of spacing. The calculations use the 17:17:17 mesh density. The differences between the isolated SR-3, the far spacing SR-3/SRV, and near spacing SR-3/SRV cases are very small. The Mach contours near the hub show a slight decrease in velocity as the spacing goes from isolated to far to near. The trailing edge shock shows a similar slight reduction in strength. The SR-3 power coefficient drops slightly with the presence of the SRV, but it increases going from far to near spacing (see the table below). In general, there is very little effect of the SRV forward on the SR-3.

The spacing effect on the SRV Mach contours is shown in figures 10 and 11. The near spacing suction surface Mach contours (fig. 10) show an increase in velocity over the entire span as compared with the far spacing contours. Only one small region (a single grid point) outboard has a Mach slightly over 1.05 at the near spacing. At the far spacing there are no grid points with a Mach number at or above 1.05. The passage Mach contours (fig. 11) are relatively low for a Mach 0.8 inflow and show that even at the near spacing there is a good hub choke margin. In fact, since the highest Mach contour crossing the passage is 0.90, the maximum Mach in the passage is lower than 0.95.

The integrated performance of these three cases is listed below. As mentioned before, the loading on the SR-3 drops in the presence of the SRV. The thrust coefficients and efficiencies for the SR-3/SRV cases are shown as (the SR-3 value)/(the SR-3 + SRV value). The $\Delta\eta$ listed is due to the increase in total thrust.

	SR-3 isolated	SR-3/Total near spacing	SR-3/Total far spacing
C_T	0.450	0.447/ 0.469	0.440/ 0.460
C_P	1.901	1.897/ 1.897	1.876/ 1.876
η, percent	77.1	76.8 /80.6	76.4 /80.0
$\Delta\eta$, percent		3.5	2.9

In order to put these efficiency improvements in perspective, the efficiency loss due to swirl from the single-rotation propfan is less than 10 percent at the design condition. This estimate is based on ideal efficiency calculations using the method of reference 10, carried out for single- and counterrotation propellers at the same operating conditions. This method will overestimate the efficiency difference because viscous losses are not accounted for.

The performance of the SRV examined here is very good. Both SRV spacings show a swirl loss recovery of roughly three percent, and so provide a significant fraction of the efficiency advantage of counter-rotation with a system only slightly more complex than single-rotation. Figure 12 shows the axisymmetric average swirl angle before and after the SRV at both the near and far axial positions. The SRV recovers roughly 40 percent of the swirl. The SRV was designed to recover about 60 percent of the swirl, so the system efficiency with the optimum blade angles should show an increase of between 4 and 5 percent.

As an aside, this design was predicted in separate work to experience flutter before reaching the design condition. The redesign, to be used in the test, will have eight blades and an increased chord length at the hub. This is estimated to reduce the efficiency recovery by about 1 percent.

CONCLUSIONS

An Euler analysis of a swirl recovery vane system was carried out to determine the system performance. There are three main points to be drawn from this work:

1. At the Mach 0.8 cruise condition, the preliminary SRV design had very little effect on the upstream propfan, even at a close spacing.

2. The SRV was able to recover about half of the efficiency loss due to swirl from the single-rotation propfan.

3. The relatively low Mach numbers in the passage of the SRV show that there is a good hub choke margin.

REFERENCES

1. Rohrback, C., Metzger, F.B., Black, D.M., and Ladden, R. M., "Evaluation of Wind Tunnel Performance Testings of an Advanced 45° Swept Eight-Bladed Propeller at Mach Numbers From 0.45 to 0.85," NASA CR-3505, 1982.

2. Neuman, H.E., Serafini, J.A., Whipple, D.Y., and Howard, B.T., "Laser-Velocimeter-Measured Flow Field Around an Advanced, Swept, Eight-Blade Propeller at Mach 0.8," NASA TP-2462, 1985.

3. Wainauski, H.S. and Vaczy, C.M., "Aerodynamic Performance of a Counter Rotating Prop-Fan," AIAA Paper 86-1550, June 1986.

4. Kroo, I., "Propeller-Wing Interaction for Minimum Induced Loss," Journal of Aircraft, Vol. 23, No. 7, July 1986, pp. 561-565.

5. Miranda, L.R. and Brennan, J.E., "Aerodynamic Effects of Wingtip-Mounted Propellers and Turbines," 4th Applied Aerodynamics Conference, AIAA, New York, 1986, pp. 221-228.

6. Patterson, J.C. Jr. and Bartlett, G.R., "Effect of a Wing-Tip Mounted Pusher Turboprop on the Aerodynamic Characteristics of a Semi-Span Wing," AIAA Paper 85-1286, July 1986.

7. Adamczyk, J.J., "Model Equation for Simulating Flows in Multistage Turbomachinery," ASME Paper 85-GT-226, Nov. 1984. (NASA TM-86869)

8. Adamczyk, J.J., Mulac, R.A. and Celestina, M. L., "A Model for Closing the Inviscid Form of the Average-Passage Equation System," ASME Paper 86-GT-227, June 1986. (NASA TM 87199)

9. Celestina, M.L., Mulac, R.A. and Adamczyk, J.J., "A Numerical Simulation of the Inviscid Flow Through A Counter-Rotating Propeller," Journal of Turbomachinery, Vol. 108, No. 4, Oct. 1986, pp. 187-193.

10. "S.B.A.C. Standard Method of Propeller Performance Estimation," Society of British Aircraft Constructors, Ltd.

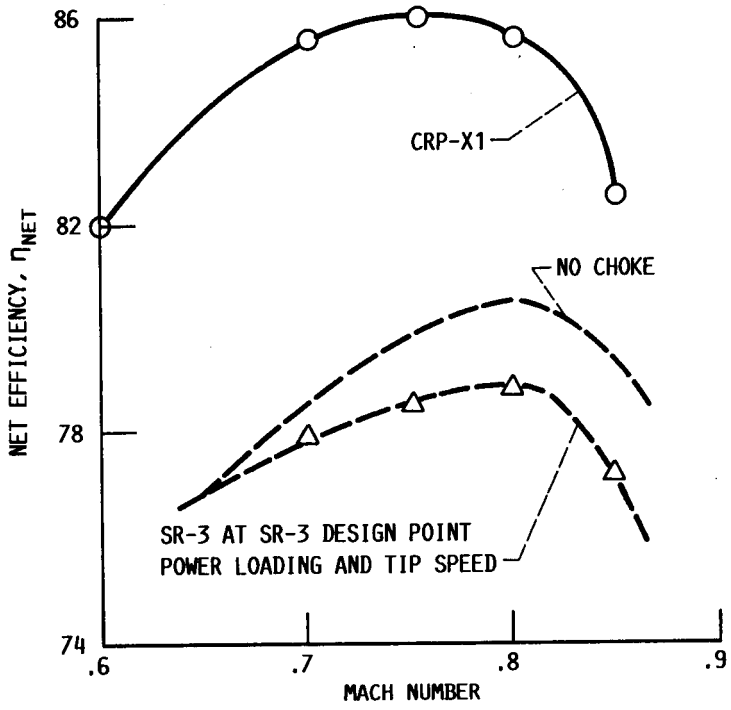

FIGURE 1. - VARIATION OF NET EFFICIENCY WITH MACH NUMBER AT DESIGN C_p AND TIP SPEED FOR SR-3 AND CRP-X1.

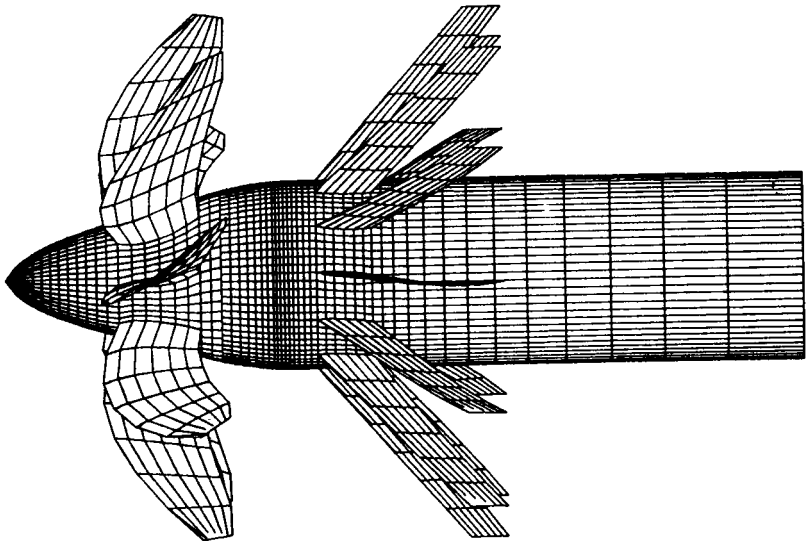

FIGURE 2. - SR-3/SRV TEST RIG AT NEAR SPACING.

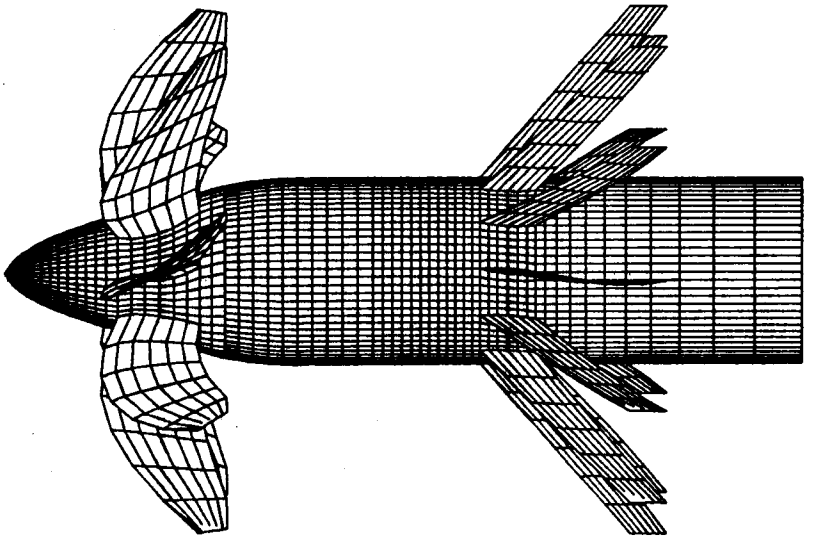

FIGURE 3. - SR-3/SRV TEST RIG AT FAR SPACING.

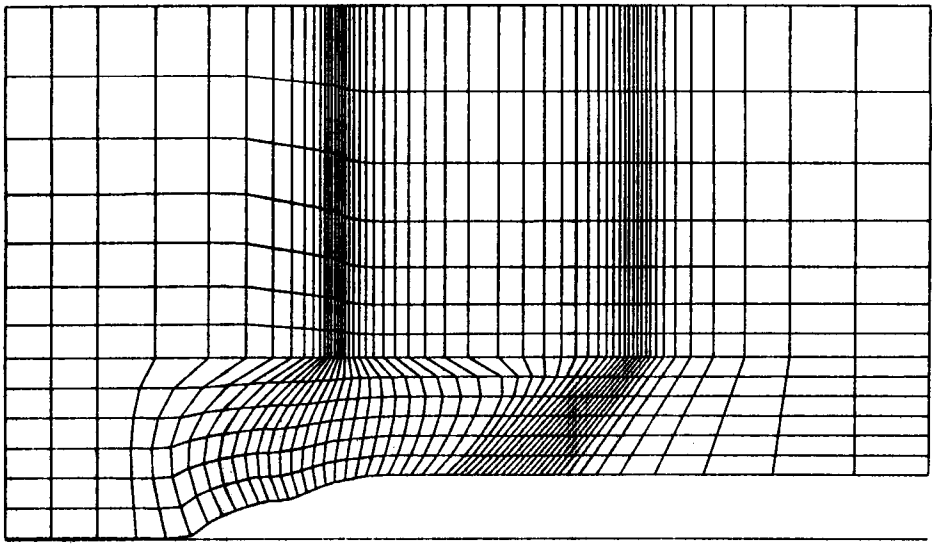

FIGURE 4. - EXAMPLE (AXIAL, RADIAL) MESH COORDINATES FOR A MESH WITH $N_a:N_r:N_c$ = 7:7:7. THE SR-3 IS LOCATED AXIALLY FROM LINES 12 TO 18. THE SRV IS AT THE FAR SPACING AND LOCATED AXIALLY FROM LINES 40 TO 46. THE TIP OF EACH BLADE IS RADIALLY AT LINE 7.

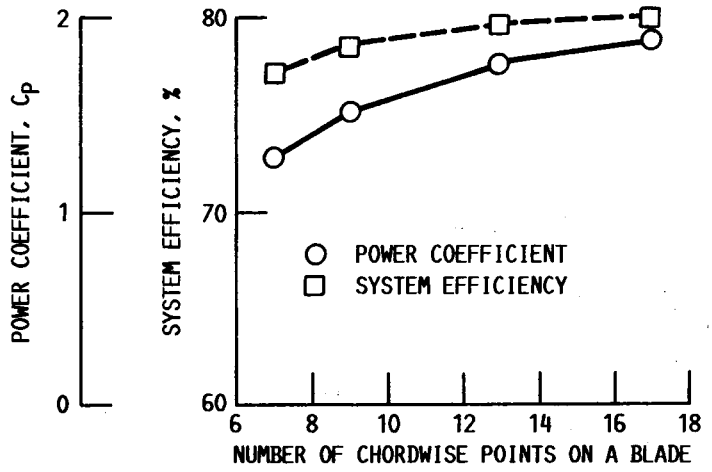

FIGURE 5.- OVERALL SR-3/SRV AERODYNAMIC PERFORMANCE VERSUS N_a AT THE FAR SPACING.

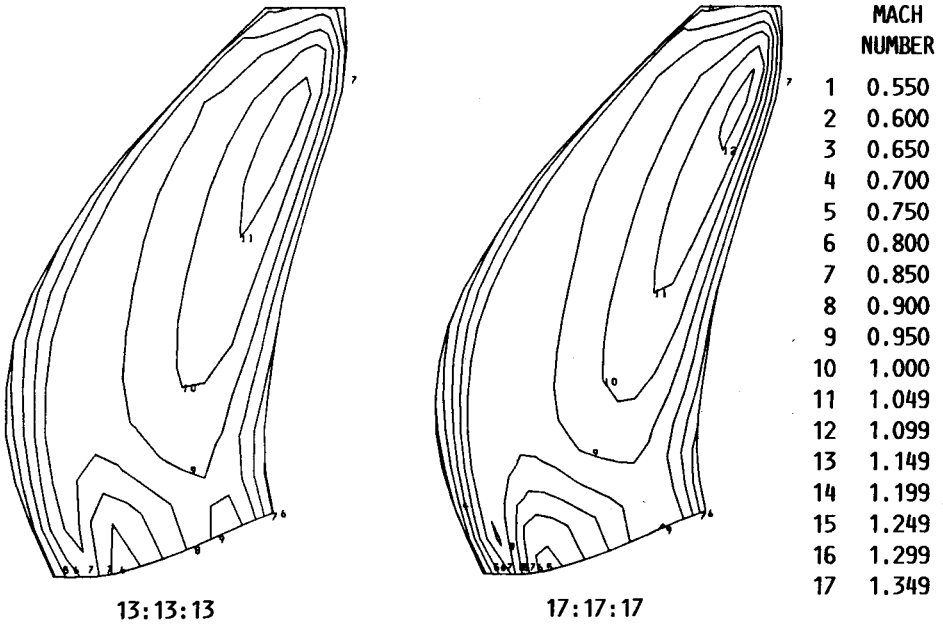

FIGURE 6. - MACH NUMBER CONTOURS ON THE SR-3 SUCTION SURFACE FOR THE 13:13:13 AND 17:17:17 MESHES. THE SRV IS PRESENT AT THE FAR SPACING.

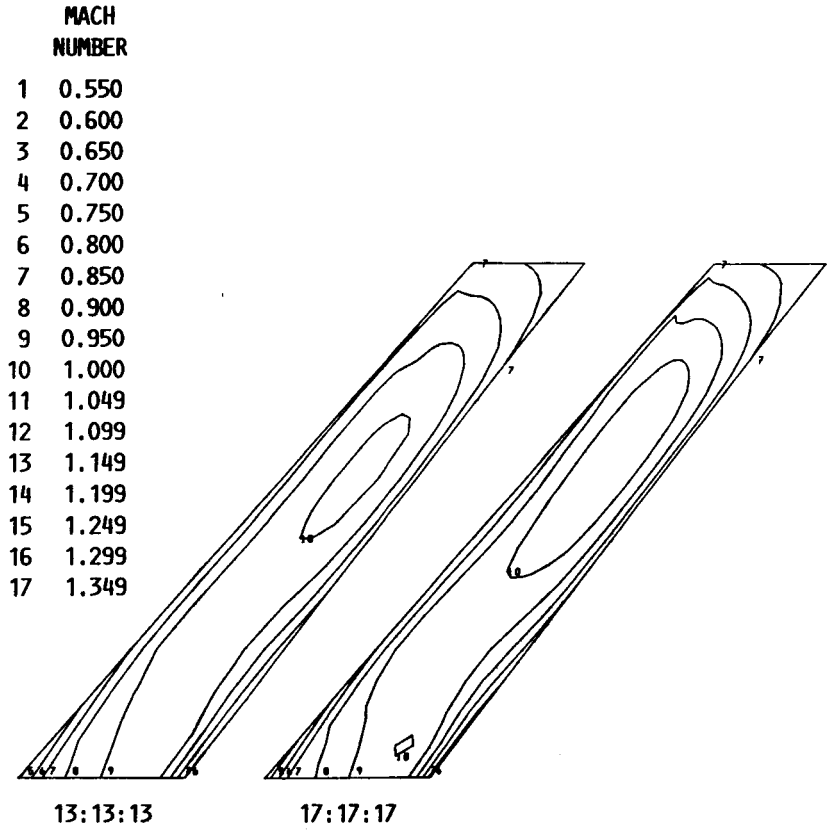

FIGURE 7. - MACH NUMBER CONTOURS ON THE SRV SUCTION SURFACE FOR THE 13:13:13 AND 17:17:17 MESHES. THE SR-3 IS PRESENT AT THE FAR SPACING.

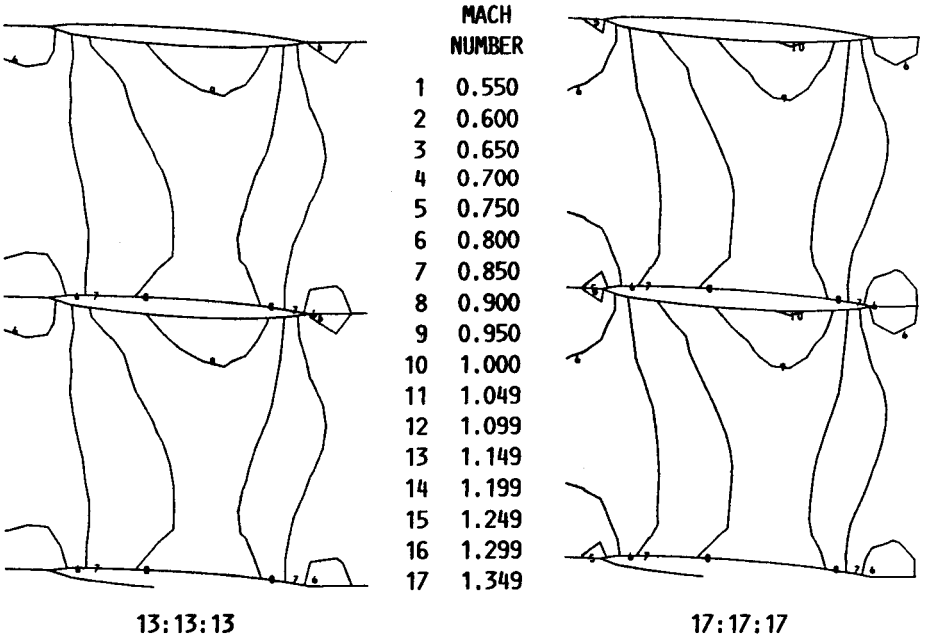

FIGURE 8. - MACH NUMBER CONTOURS IN THE PASSAGE OF THE SRV AT THE FIRST GRID SURFACE OFF THE HUB WITH THE 13:13:13 AND 17:17:17 MESHES. THE SR-3 IS PRESENT AT THE FAR SPACING.

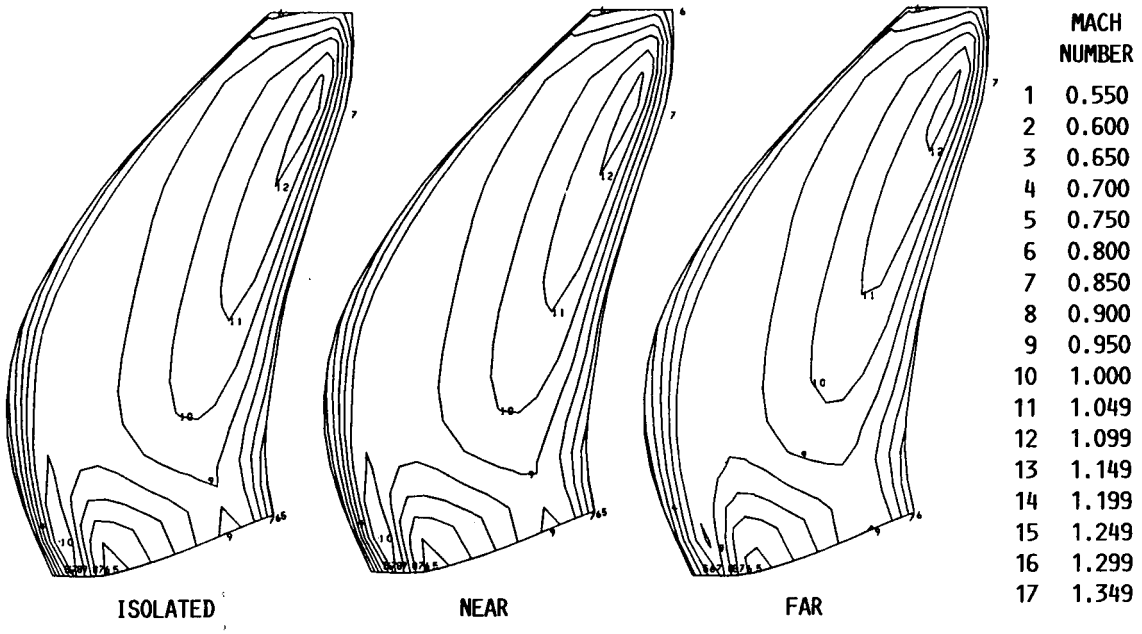

FIGURE 9. - MACH NUMBER CONTOURS ON THE SR-3 SUCTION SURFACE FOR THE ISOLATED, NEAR, AND FAR SPACING CONFIGURATIONS. THE MESH PARAMETERS ARE 17:17:17.

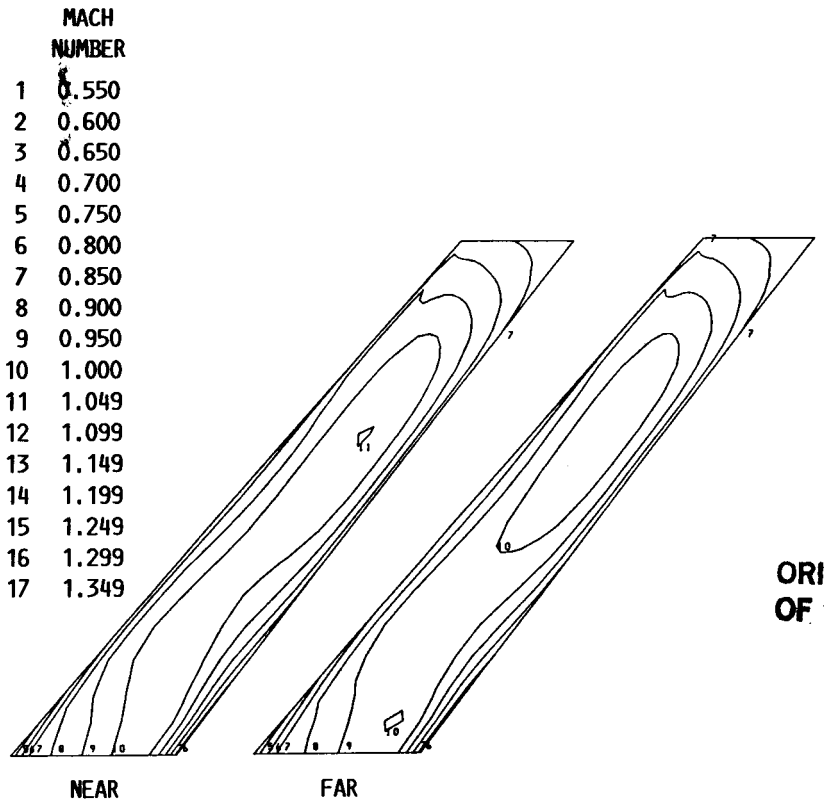

FIGURE 10. - MACH NUMBER CONTOURS ON THE SRV SUCTION SURFACE FOR THE NEAR AND FAR SPACING CONFIGURATIONS. THE MESH PARAMETERS ARE 17:17:17.

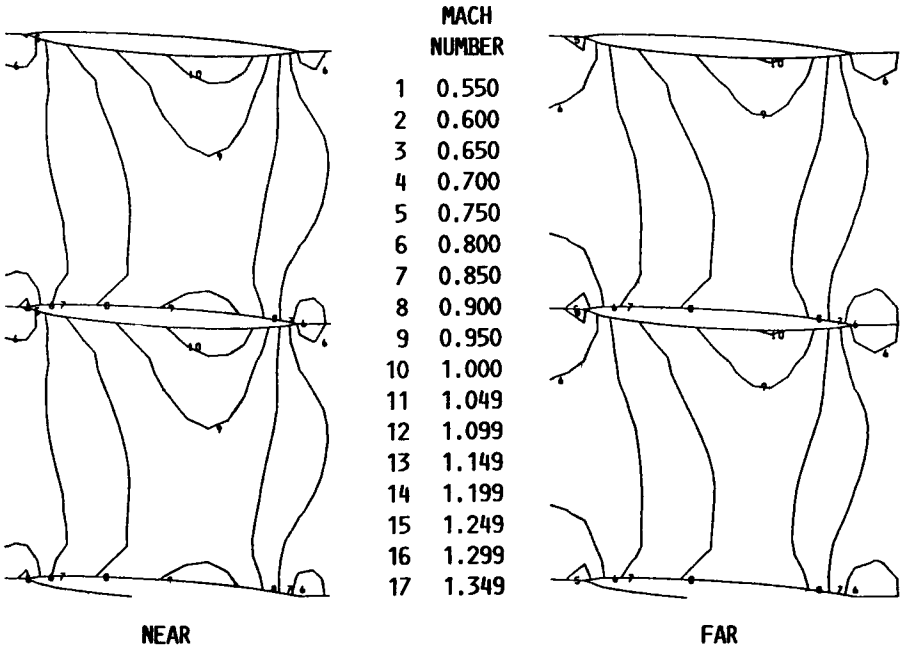

FIGURE 11. - MACH NUMBER CONTOURS IN THE SRV PASSAGE AT THE FIRST GRID SURFACE OFF THE HUB FOR THE NEAR AND FAR SPACING CONFIGURATIONS. THE MESH PARAMETERS ARE 17:17:17.

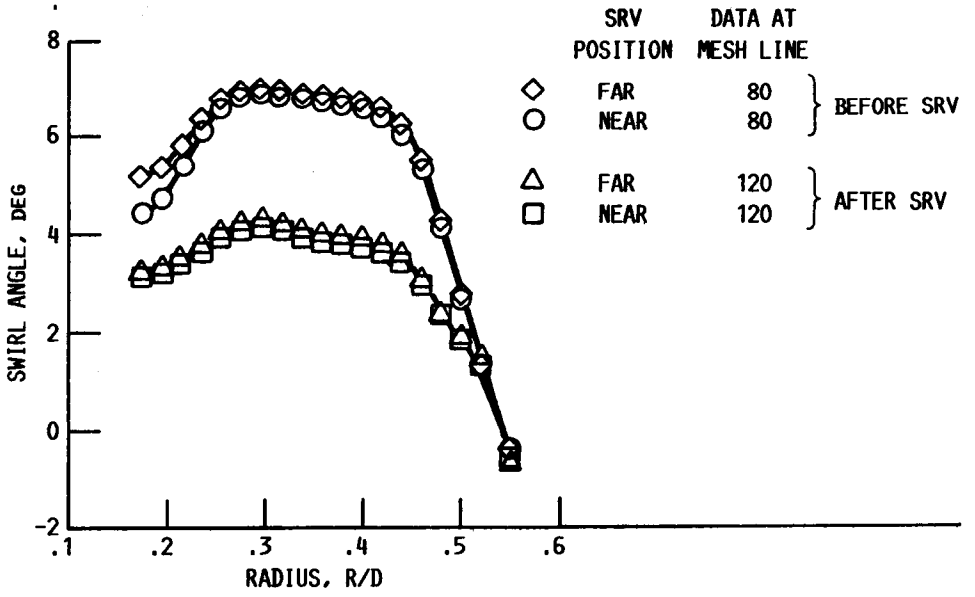

FIGURE 12. - RADIAL DISTRIBUTION OF THE AXISYMMETRICALLY AVERAGED SWIRL ANGLE BEFORE AND AFTER THE SRV FOR THE NEAR AND FAR AXIAL SPACINGS.

NASA
National Aeronautics and Space Administration

Report Documentation Page

1. Report No.	2. Government Accession No.	3. Recipient's Catalog No.
NASA TM-101357 AIAA-88-3152		

4. Title and Subtitle

Euler Analysis of a Swirl Recovery Vane Design for Use With an Advanced Single-Rotation Propfan

5. Report Date

6. Performing Organization Code

7. Author(s)

Christopher J. Miller

8. Performing Organization Report No.

E-4387

10. Work Unit No.

535-03-01

9. Performing Organization Name and Address

National Aeronautics and Space Administration
Lewis Research Center
Cleveland, Ohio 44135-3191

11. Contract or Grant No.

13. Type of Report and Period Covered

Technical Memorandum

12. Sponsoring Agency Name and Address

National Aeronautics and Space Administration
Washington, D.C. 20546-0001

14. Sponsoring Agency Code

15. Supplementary Notes

Presented at the 24th Joint Propulsion Conference cosponsored by the AIAA, ASME, SAE, and ASEE, Boston, Massachusetts, July 11-13, 1988.

16. Abstract

Recent work has demonstrated the propulsive efficiency improvements available from single- and counter-rotation propfans as compared with current technology high bypass ratio turbofans. This paper examines the concept known as swirl recovery vanes (SRV) through the use of a three-dimensional Euler code. At high speed cruise conditions, the SRV can improve the efficiency level of a single-rotation propfan, but a concern is to have adequate hub choke margin. The SRV was designed with two-dimensional methods and was predicted to have hub choking at a Mach 0.8 cruise. The three-dimensional Euler analysis properly accounts for sweep effects and three-dimensional relief, and predicts that at cruise the SRV will recover roughly 5 percent of the 10 percent efficiency loss due to swirl and have a good hub choke margin.

17. Key Words (Suggested by Author(s))	18. Distribution Statement
Propeller Transonic efficiency	Unclassified – Unlimited Subject Category 02

19. Security Classif. (of this report)	20. Security Classif. (of this page)	21. No of pages	22. Price*
Unclassified	Unclassified	14	A03

*For sale by the National Technical Information Service, Springfield, Virginia 22161